

BEHAVIOR OF NANOCRYSTALLINE Xe PRECIPITATES IN Al UNDER 1 MeV ELECTRON IRRADIATION*

C. W. Allen¹, M. Song², K. Furuya², R. C. Birtcher¹,
S. E. Donnelly³, and K. Mitsuishi²

¹Materials Science Division
Argonne National Laboratory
9700 S. Cass Ave.
Argonne, IL 60439

²National Research Institute for Metals
Tsukuba, Ibaraki 305-0003, Japan

³University of Salford
Manchester M5 4WT, UK

February 1999

The submitted manuscript has
been created by the University of
Chicago as Operator of Argonne
National Laboratory ("Argonne")
under Contract No. W-31-109-
ENG-38 with the U.S. Department
of Energy. The U.S. Government
retains for itself, and others
acting on its behalf, a paid-up,
non exclusive, irrevocable
worldwide license in said article
to reproduce, prepare derivative
works, distribute copies to the
public, and perform publicly and
display publicly, by or on behalf
of the Government.

RECEIVED
OCT 13 1999
OSTI

Paper to be submitted to the Structures and Properties of Multi-Lattice Materials, Tsukuba,
Japan, February 3-5, 1999.

*Work supported by the U. S. Department of Energy, Office of Basic Energy Sciences, under
Contract W-31-109-Eng-38 at Argonne National Laboratory, NATO grant No. 910670, and by the
Science and Technology Agency of Japan.

DISCLAIMER

This report was prepared as an account of work sponsored by an agency of the United States Government. Neither the United States Government nor any agency thereof, nor any of their employees, make any warranty, express or implied, or assumes any legal liability or responsibility for the accuracy, completeness, or usefulness of any information, apparatus, product, or process disclosed, or represents that its use would not infringe privately owned rights. Reference herein to any specific commercial product, process, or service by trade name, trademark, manufacturer, or otherwise does not necessarily constitute or imply its endorsement, recommendation, or favoring by the United States Government or any agency thereof. The views and opinions of authors expressed herein do not necessarily state or reflect those of the United States Government or any agency thereof.

DISCLAIMER

**Portions of this document may be illegible
in electronic image products. Images are
produced from the best available original
document.**

Behavior of nanocrystalline Xe precipitates in Al under 1 MeV electron irradiation

C. W. Allen^{1,*}, M. Song², K. Furuya², R. C. Birtcher¹, S. E. Donnelly³ and K. Mitsuishi²

¹Argonne National Laboratory, Argonne, IL 60439, USA

²National Research Institute for Metals, Tsukuba, Ibaraki 305-0003, JAPAN

³University of Salford, Manchester M5 4WT, UK

***Corresponding Author:**

Dr. Charles W. Allen
Materials Science Division—Building 212/E211
Argonne National Laboratory
9700 South Cass Avenue
Argonne, IL 60439 USA
Phone: (630) 252-4157
FAX: (630) 252-4798
E-Mail: allen@aaem.amc.anl.gov

Running Title:

Xe precipitates in Al

Key Words:

high-resolution electron microscopy, Al, Xe precipitate, irradiation, nanocrystal

Total Number of Pages Submitted (including this cover page): 11

Total Number of Figures Submitted: 5

Behavior of nanocrystalline Xe precipitates in Al under 1 MeV electron irradiation

C. W. Allen^{1,*}, M. Song², K. Furuya², R. C. Birtcher¹, S. E. Donnelly³ and K. Mitsuishi²

¹Argonne National Laboratory, Argonne, IL 60439 USA, ²National Research Institute for Metals, Tsukuba, Ibaraki 305-0003, JAPAN and ³University of Salford, Manchester M5 4WT, UK

*To whom correspondence should be addressed

Abstract Crystalline nanoprecipitates of Xe have been produced by ion implantation into high purity Al at 300 K. With an off-zone axis TEM imaging technique, the nanocrystals may be clearly structure imaged against a nearly featureless background. Under the 1 MeV electron irradiation employed for the HREM observation, Xe nanocrystals exhibit a number of readily observed physical phenomena including migration within the matrix, changes in shape, faulting, melting, crystallization and coalescence. The various phenomena observed as changes in the Xe nanocrystals reflect changes of matrix cavity-surface structure. The Xe nanocrystal thus allows investigation indirectly into changes in interface morphology at the atomic level, resulting in this instance from electron irradiation damage. Such changes have heretofore been inaccessible to observation.

Keywords high-resolution electron microscopy, Xe precipitate, irradiation, nanocrystal

Received

Introduction

The implantation of noble gases into metal matrices results in a fine dispersion of precipitates of the implanted species. Such precipitates may be crystalline or noncrystalline depending on their sizes and the observation temperature. It is not unusual for nanometer-sized precipitates to be crystalline at temperatures as high as 600 K. For example, this is the case for Xe precipitates in Al even though the triple point for Xe is approximately 160 K. The generally accepted origin for this phenomenon is the surface tension γ of the matrix/precipitate interface which results in compression of the precipitate, the magnitude of which is a function of the precipitate size. In the isotropic approximation, this compressive stress $|\sigma| = 2\gamma/R$ where R is the radius of a spherical precipitate and γ is interfacial tension. In crystalline matrices, the noble gas precipitates are generally not spherical but rather polyhedral. For noble gases in fcc matrices, precipitates assume the shape of matrix voids, usually $\{100\}$ cubes with deep truncations of the corners, parallel to $\{111\}$ (cuboctahedra). The crystalline precipitates are close-packed (fcc in fcc matrices) with lattice parameters much larger than those of the host; e.g., the lattice parameter of Xe is approximately 1.5 times that of Al [1]. As a consequence the precipitate/matrix interface is incommensurate, while the lattices nevertheless are isotactic. The Xe lattice parameter increases slightly with increasing precipitate size, the Xe evidently obeying its equation of state under the influence of the interfacial tension of the matrix cavities [2].

Under Frenkel pair-producing electron irradiation, Al-Xe alloys are driven far enough from equilibrium that a number of dynamic phenomena involving the Xe precipitates are observed, including melting and crystallization, faulting and layer shuffling, precipitate migration, and coalescence [3-5]. Observed in transmission electron microscopy under high-resolution conditions with respect to the Xe, results of studies of such phenomena are informative not only with respect to the properties of the Xe precipitates but also with respect to radiation-induced changes on the matrix cavity surfaces, which are directly responsible for the observed changes in the precipitates.

The purpose of this paper is to present a brief summary of observed radiation-induced phenomena in the Xe, both in the crystalline form and in a non-crystalline state. The experiments were performed *in situ* in a high-resolution high-voltage electron microscope in which realtime observations of precipitate behavior were video recorded during the electron irradiation. An earlier paper in this journal examined the morphologies of a dispersion of Xe precipitates in mazed bicrystalline Al, with

particular emphasis on the structure and behavior of the Xe at and near 90° tilt boundaries on which the Xe precipitates are bicrystals [6].

Materials and methods

Transmission electron microscopy (TEM) specimens were prepared at Argonne National Laboratory by jet electropolishing of well annealed 5N Al. Specimens were then implanted with 35 keV Xe to a dose of $2-4 \times 10^{19} \text{ m}^{-2}$. A Monte Carlo simulation for the implantation conditions by TRIM 95 [7] yields a mean depth for the implanted Xe of 25 nm. Electron irradiations and high resolution imaging were performed simultaneously in the JEOL ARM-1000 high voltage electron microscope (HVEM) at the High Resolution Beam Station of the National Research Institute for Metals (NRIM), Tsukuba, Japan. The HVEM was operated at 1 MeV with a LaB₆ electron source. 1 MeV electron irradiations were performed with a focused electron beam, without a condenser aperture. The peak electron flux at the specimen was typically $6.6 \times 10^{24} \text{ m}^{-2} \text{s}^{-1}$. With a displacement cross-section for Al by 1 MeV electrons of $60 \times 10^{-28} \text{ m}^{-2}$ [8], the corresponding Al displacement rate was 3.9×10^{-2} displacements per Al atom per sec (dpa·s⁻¹). It was found that good structure imaging of Xe precipitates could be achieved with the intense electron beam during the irradiation so that resulting structural changes in the Xe could be observed in real time [9].

The point-to-point resolution limit of NRIM ARM-1000 is 0.13 nm. For high resolution imaging at 1 MeV, Scherzer defocus is 57 nm [5]. In order to decrease the contrast of the Al matrix relative to that of the Xe precipitates, a variation of the method of Tanaka et al. was adopted [10]. The specimen was tilted approximately 3 degrees off a <110> zone axis about a 115 reciprocal lattice vector, and the objective lens was defocused to a value at which the contrast transfer function for low order Al spacings was near zero. Because of the small size and larger lattice parameter of the Xe crystals, the Xe structure images were not noticeably degraded by this off-axial imaging technique, in agreement with image simulations [9]. The high resolution image was video tape recorded continuously (S-VHS) in real time at 30 frames per second with a running 3 or 5 frame average.

The specimen orientation employed, therefore, is very near [110] as represented in the sketch, Fig.1, which shows an assembly of Xe cuboctahedra viewed along [110]. The TEM images are projections of such assemblies.

Results and discussion

Electron irradiation creates many changes in the microstructure of the Al (Xe) specimens. In the as-implanted condition, the Xe precipitates have somewhat irregular facets on {100} and {111} faces. Electron irradiation, through atomic displacements at the interface, the migration of point defects to the interface, and/or impingement of Frank loops from the Al matrix, causes fluctuations in the roughness of the matrix/precipitate interfaces, to which the Xe precipitates respond in a variety of ways. Such fluctuations seem to be fundamental to all of the changes which the Xe precipitates experience. At the electron flux employed here ($6.6 \times 10^{24} \text{ m}^{-2} \text{s}^{-1}$), the damage rate in the alloy is large; the Al matrix experiences 1 dpa per 25 sec, approximately (i.e., on average each Al atom in the bulk is displaced once every 25 sec). Whether or not the Xe experiences direct displacement by 1 MeV electrons is not known.

Fig. 2 details the shape changes and motion of a nanometer size, solid Xe precipitate in Al during electron irradiation at room temperature over an increment of 11.5 dpa. All precipitates in Fig. 2 exhibit some relative motion and shape change. Because of its size, the small Xe precipitate at center, composed of 14–15 Xe atom columns, exhibits the largest amount of motion. Initially one has the impression, from Figs 2(b) and (c), for instance, that the precipitate size is changing but one must remember that he sees only fluctuations in the plane of projection; any fluctuations in [110], the specimen orientation, go largely unnoticed. A second consideration is the number of Xe atoms in each column for such a small precipitate. An ideal atomic cuboctahedron of minimum size contains 14 atom columns and a total of 38 Xe atoms. The number of Xe atoms per column ranges from 2–4. By comparison, in a 50 nm thick region of <110> Al there are about 178 Al atoms per column. Thus the sensitivity of observation of Xe by the off-axial imaging technique is really quite extraordinary.

To judge from observation of a number of small crystalline precipitates, the size does not change during electron irradiation, indicating that an equal number of Al interstitials and vacancies arrive and recombine at the interface and no Xe is added or subtracted. In effect the motion must be due to the net transport of Al from one part of the precipitate/matrix interface to another. The arrival of defects will not result in motion of the precipitate unless there is a directional bias in the defect absorption and

recombination that results in such differential transport. The random nature of the motion of small, relatively isolated precipitates suggests that this is not the case.

Fig. 3 shows two larger Xe precipitates from the same video area as Fig. 2, which are moving toward one another. Other precipitates in the neighborhood are also moving. It is likely that such non-random migration is due to the net displacement of Al out of the region between the two adjacent precipitate particles. When coalescence results from such non-random motion, this process has been termed 'sputter coalescence' and reported for He bubbles in Al [12]. Inspection of the various particle edges in the sequence of Fig. 3 (the edges in the images are two sets of $\{111\}_{\text{Xe}}$ and one set of $(001)_{\text{Xe}}$) reveals Xe ledges on these interfaces which must be associated with ledges on the Al cavity surfaces.

An unusual, simultaneous coalescence of three non-crystalline Xe precipitates is shown in Fig. 4. Unfortunately a significant part of the process occurs off-screen so that much detail is missed. The sequence illustrates well, however, the rapidity with which noncrystalline Xe precipitates change shape and coalesce at room temperature under electron irradiation. In this case the irradiation-induced diffusion of Al involves a large number of Al atoms over the bulk Al dose-interval of about 1dpa. The coalescence of two non-crystalline Xe precipitates [11] and of two crystalline precipitates [13] have been discussed elsewhere.

Fig. 5 shows a sequence in which a Xe precipitate which is initially crystalline, Figs. 5(a) and (b); has melted, Fig. 5(c); proceeds to crystallize again, Fig. 5(d); later appears to be partially melted, Fig. 5(f), in the process of melting again under the influence of the electron irradiation. In this case, the difference in volume of the precipitate as crystalline, Fig. 5(b), and non-crystalline, Fig. 5(d), is approximately 30 percent. Non-crystalline Xe precipitates may or may not change volume over their lifetime, depending on factors which at this point remain obscure.

When the shape of an Al cavity changes, the Xe lattice often conforms by imperfect or partial slip on $\{111\}_{\text{Xe}}$ (i.e., due to glide of Shockley-like partial dislocations in the Xe), as illustrated in Fig. 5(a). By Fig. 5(b), the fault has disappeared. A similar fault appears in Fig. 5(d) following recrystallization of the precipitate. The behavior of such faults has been described previously [3-6].

In addition to faulting of the fcc Xe, occasionally shuffles on $\{111\}_{\text{Xe}}$ also appear, which in this structure are not so easily understood. The phenomenon is not illustrated here but consists of a single $\{111\}_{\text{Xe}}$ layer shifting back and forth before falling back into the proper fcc stacking sequence; then an adjacent layer may behave similarly and so on until the process reaches the matrix interface. If the Xe were close-packed

hexagonal, such layer shuffling could be understood geometrically in the usual way (in a sequence ...ABAB..., a B-layer could shuffle between C and B-layer positions without violating nearest neighbor relations, but in fcc this is not geometrically possible without neighboring layers such as CC forming which involve nearest neighbor violations).

The mechanism of layer shuffling in fcc is also obscure at this point.

While changes, such as faulting or shuffling, on two of the four sets of $\{111\}_{\text{Xe}}$ are clearly imaged in the near [110] foil orientation, such changes on the other two 111 sets which are inclined by about 55 deg to the vertical may confuse portions of the Xe images and their interpretation.

The last phenomenon which we shall mention is the abrupt disappearance of Xe precipitates at free surfaces. The relative roles of electron-induced sputtering of Al (the surface moves to the precipitate) and defect-induced migration of the precipitate (the precipitate moves to the surface) are not clear because imaging in this foil orientation does not permit changes resulting in movement of surfaces or precipitates in [110] to be observed. It is observed frequently that Xe precipitates suddenly disappear after 200 dpa or so, leaving a crater which heals in a matter of seconds at room temperature during the irradiation.

Concluding remarks

From this overview of irradiation-induced phenomena in the Xe-Al system the following points emerge. In the electron radiation environment, growth of Xe precipitates, following Xe implantation, is achieved mainly by migration and coalescence of Xe precipitates, not by an Ostwald ripening mechanism. Much of the modelling of migration of gas bubbles in irradiation environments has assumed that only those which are non-crystalline migrate [14]. It is clear, however, at least in the irradiation environment of these experiments, that both crystalline and non-crystalline Xe precipitates migrate, even at ambient temperature. Both crystalline and non-crystalline Xe precipitates also undergo dynamic shape changes, however these changes tend to be more exaggerated for the non-crystalline precipitates, the volume of which may vary significantly. These phenomena are of immediate relevance to problems involving gases in materials in irradiation environments.

The various observed phenomena are intimately interrelated, the common denominator being irradiation-induced changes in matrix/precipitate interface topography. While the main focus here has been on the behavior of the Xe precipitates, this behavior is really a reflection of structural surface changes on the Al cavity which confines the Xe precipitate. Thus, the Xe acts as a kind of tracer of

irradiation-associated changes of the Al cavity surfaces, changes which heretofore have not been deducible from observation, directly or indirectly.

Finally, the Xe precipitates exist at 300 K because of the surface tensions of the Al cavities which confine them. It has been estimated from Xe lattice parameters that Xe in the solid state is stabilized at 300 K by an equilibrium pressure of the order of 1 GPa [1]. To balance this, the Xe interatomic forces are highly repulsive. As judged from changes of Xe lattice parameter with precipitate size, crystalline Xe exhibits large compressibility, nonetheless, which is a major distinguishing characteristic compared to more common nanoprecipitates in such matrices, which exhibit metallic, ionic or covalent bonding. At the same time, the behavior of Xe nanoprecipitates, which we have shown is relatively easy to observe at high resolution, lends insight, nevertheless, to understanding of the behavior of other more common, constrained nanoparticle systems, the large compressibility and lattice parameter of Xe exaggerating its behavior to a significant extent.

Acknowledgments

The authors are indebted especially to several individuals at Argonne National Laboratory: Bernard Kestel and Loren Funk for specimen preparation and ion implantation and Edward Ryan for assistance in preparation of Figures. This work was performed under the Japan-USA Scientific Exchange Agreement and was supported at the respective laboratories of the authors by the US Department of Energy under Contract Nos. W-31-109-Eng-38 (ANL) and by the Science and Technology Agency of Japan, for which the authors are very grateful. Two of the authors (RCB, SED) also acknowledge support from NATO in the form of a collaborative research grant No. 910670.

References

- 1 Templier C (1991) Inert gas bubbles in metals. In: *Fundamental Aspects Of Inert Gases in Solids*, ed. Donnelly S E and Evans J H, pp. 117–132 (Plenum Press, New York).
- 2 Liu A S, and Birtcher R C (1989) Precipitation of Ar, Kr and Xe in Ni at room temperature. In: *Processing and Characterization of Materials Using Ion Beams* (MRS Symposium vol. 128), ed. Rehn L E, Greene J, and Smidt F A, pp. 303–308 (Materials Research Society, Pittsburgh).
- 3 Donnelly S E, Furuya K, Song M, Birtcher R C and Allen C W (1999) 1 MeV electron irradiation of solid Xe nanoclusters in Al: an in-situ HRTEM study. In: *Proceedings of International Centennial Symposium on the Electron*, Cambridge, UK. In Press.
- 4 Mitsuishi K, Song M, Furuya K, Birtcher R C, Allen C W and Donnelly S E (1998) In-situ observation of atomic processes in Xe nanocrystals embedded in Al. In: *Atomistic Mechanisms in Beam Synthesis and Irradiation of Materials* (MRS Symposium vol. 504), ed. Barbour J C, Ila D, Roorda S and Tsugioka M, pp. (Materials Research Society, Pittsburgh). In Press.
- 5 Ishikawa N, Awaji M, Furuya K, Birtcher R C and Allen C W (1997) HRTEM analysis of solid precipitates in Xe-implanted aluminum. *Nucl. Instr. Meth. Phys. Res B* **127/128**, 123–126.
- 6 Allen C W, Song M, Furuya K, Birtcher R C, Mitsuishi K and Dahmen U (1999) Xe precipitates at grain boundaries in Al under 1 MeV electron irradiation. Submitted to: *J. Electron Microscopy*.
- 7 Ziegler J F, Biersack P J, and Littmark U (1985) *The Stopping and Range of Ions in Solids*, ed. Ziegler J F (Pergamon Press, New York).
- 8 Lucasson P G and Walker R M (1962) Production and recovery of electron-induced radiation damage in a number of metals. *Phys. Rev.* **127**, 485–500.
- 9 (a) Furuya K, Song M, Mitsuishi K, Birtcher R C, Allen C W and Donnelly S E (1999) Direct imaging of atomic structure of Xe nanocrystals embedded in Al. In:

Proceedings of International Centennial Symposium on the Electron, Cambridge, UK. In Press. (b) Furuya K, Ishikawa N and Allen C W (1999) In-situ determination of shape and atomic structure of Xe nanocrystals embedded in aluminum. *J. of Micros.* In Press.

10 (a) Tanaka N, Nagao M and Mihami K (1988) High resolution electron microscopy of composite films of gold and magnesium oxide. *Ultramicroscopy* **25**, 241–252.
(b) Tanaka N, Kimoto K and Mihami K (1991) Observations in HVEM of atomic clusters embedded in MgO crystals. *Ultramicroscopy* **39**, 395–402.

11 Allen C W, Birtcher R C, Donnelly S E, Furuya K, Ishikawa N, and Song M (1999) Migration and coalescence of Xe nanoprecipitates in Al induced by electron irradiation at 300 K. Submitted to: *Appl. Phys. Lett.*

12 Birtcher R C, Donnelly S E and Templier C (1994) Evolution of helium bubbles in aluminum during heavy-ion irradiation. *Phys. Rev. B1* **50**, 764–769.

13 Birtcher R C, Donnelly S E, Song M, Furuya K, Mitsuishi K and Allen C W (1997) Coalescence of solid Xe precipitates in Al. Submitted to: *Phys. Rev. B1*.

14 Rest J and Birtcher R C (1989) Precipitation kinetics of rare gases implanted into metals. *J. Nucl. Mater.* **168**, 312–325.

Figure captions

Figure 1. Assembly of cuboctahedra composed of {100} (four sided) and {111} (six sided) faces, viewed down [110].

Figure 2. Shape changes and motion of a nm size, solid Xe precipitate in [110] Al during 1 MeV electron irradiation at room temperature. Accumulated electron doses from the first frame are (b) 1.9, (c) 9.5 and (d) $19.4 \times 10^{26} \text{ m}^{-2}$ corresponding to accumulated damage from the first frame of (b) 1.1, (c) 5.6 and (d) 11.5 dpa.

Figure 3. Shape changes and motion of 10 nm size solid Xe precipitates in [110] Al during 1 MeV electron irradiation at room temperature. The accumulated electron doses from the first frame are (b) 13.2, (c) 27.4 and (d) $32.8 \times 10^{26} \text{ m}^{-2}$ corresponding to accumulated damage from the first frame of (b) 7.8, (c) 16.2 and (d) 19.4 dpa.

Figure 4. Formation of large Xe precipitate by the coalescence of several smaller ones during 1 MeV electron irradiation at room temperature. Electron doses after 16.2 and 24.4 seconds correspond to additional damage accumulation of 0.63 and 0.95 dpa.

Figure 5. Examples of structural changes of single Xe precipitate in [110] Al during 1 MeV electron irradiation at room temperature. Original stacking fault (a) through the precipitate is removed (b, 0.4 dpa). After some time the precipitate melts (c, 12.2 dpa) and then resolidifies (d, 15.2 dpa) incorporating a stacking fault that is subsequently removed (e, 15.6 dpa). (f, 32.1 dpa) precipitate has partially melted and a second precipitate that is partially visible at top of each frame has disappeared. At no time do all facets of precipitate appear to be flat.

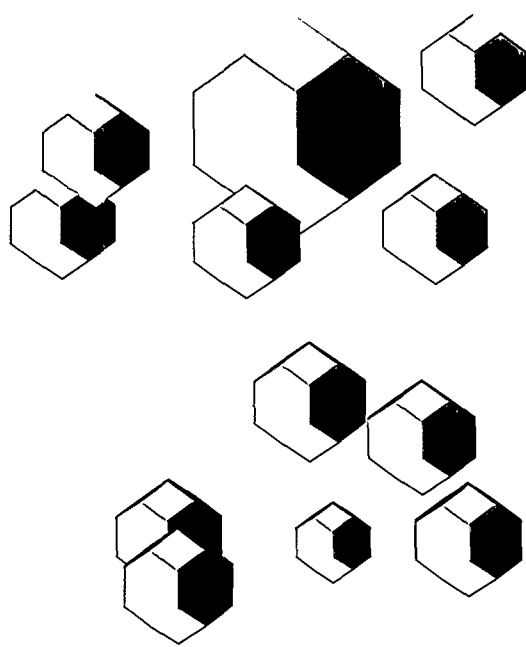


FIG.1

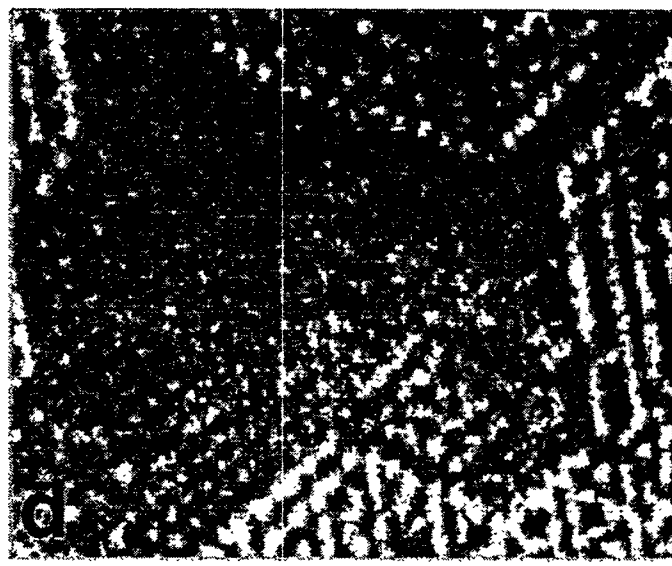
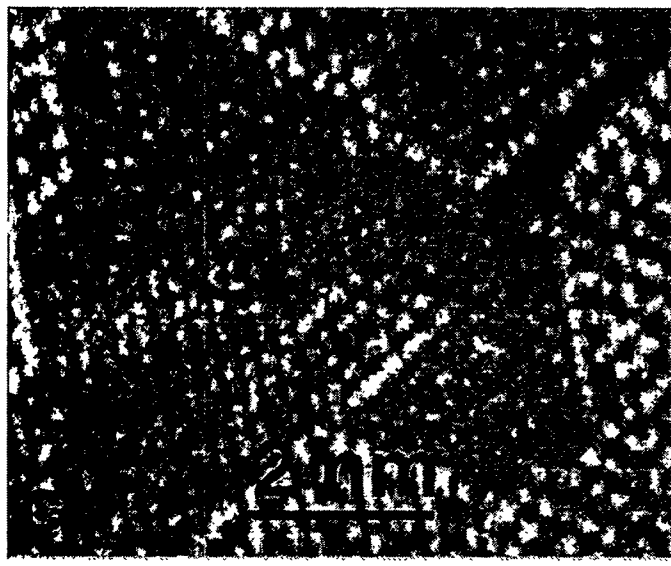
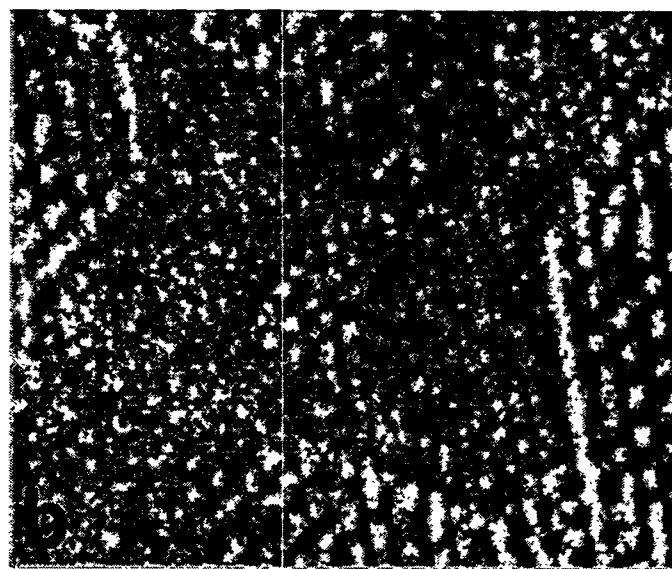
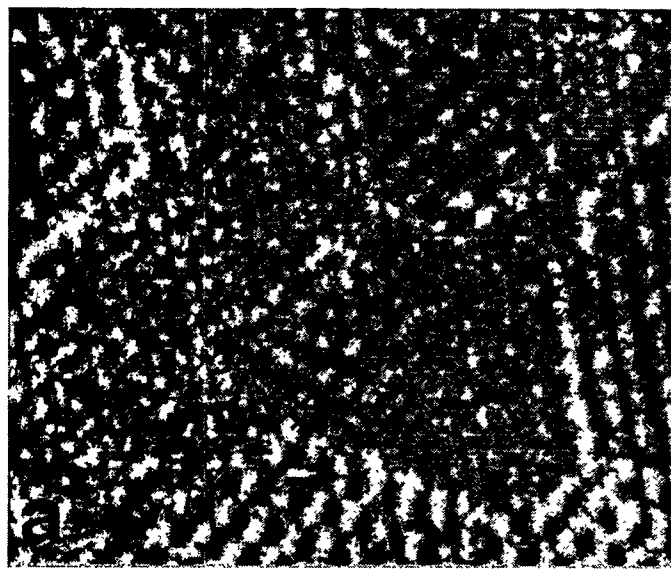


FIG. 2

